Chemical Geology 602 (2022) 120899

Contents lists available at ScienceDirect

Chemical Geology

journal homepage: www.elsevier.com/locate/chemgeo

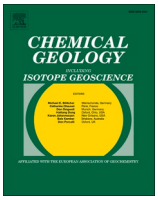

Iron isotope compositions of subduction-derived rocks: Insights from eclogites and metasediments of the Münchberg Massif (Germany)

Johannes E. Pohlner [a,*], Afifé El Korh [a], Massimo Chiaradia [b], Reiner Klemd [c], Bernard Grobéty [a], Thomas Pettke [d]

[a] Unit of Earth Sciences, Department of Geosciences, University of Fribourg, Chemin du Musée 6, 1700 Fribourg, Switzerland
[b] Department of Earth Sciences, University of Geneva, Rue des Maraîchers 13, 1205 Geneva, Switzerland
[c] GeoZentrum Nordbayern, Universität Erlangen-Nürnberg, Schlossgarten 5a, 91054 Erlangen, Germany
[d] Institute of Geological Sciences, University of Bern, Baltzerstrasse 1+3, 3012 Bern, Switzerland

ARTICLE INFO

Editor: Catherine Chauvel

Keywords:
Eclogites
Fe isotopes
Subduction
Fluid-rock interactions

ABSTRACT

The Fe isotope systematics of subducted lithologies are crucial for the understanding of redox-dependent mass transfer in subducting slabs, with consequences for the compositions of arc magmas and of the deep mantle. We investigated eclogites, metagabbros, and paragneisses from the Variscan Münchberg Massif to unravel whether their Fe isotope compositions are dominated by the igneous/sedimentary protolith signature, by low-temperature seawater alteration, or by later fluid-rock interactions during the subduction-exhumation cycle. Although the eclogites are thought to be derived from a continental rather than oceanic setting (possibly a rift-drift transition stage), they have mid-ocean ridge basalt (MORB)-like major and trace element compositions. They are often moderately oxidized compared to MORB ($Fe^{3+}/\Sigma Fe$ = 0.06 to 0.30). Their $\delta^{56}Fe$ values (+0.00 to +0.17‰; mean + 0.08 ± 0.01‰) mostly resemble those of MORB (+0.07 to +0.17‰). The metagabbros, which are derived from a more enriched mantle source than the eclogites, yielded heavier $\delta^{56}Fe$ values (+0.09 to +0.22‰) similar to ocean island basalts, whereas those of the paragneisses (+0.03 to +0.10‰) are typical for pelitic sediments.

It appears that the Fe isotope compositions of the igneous protoliths are largely preserved and little if any Fe was mobilized during the diverse fluid-rock interaction stages. The parental magma of the eclogites was probably somewhat isotopically lighter than similarly differentiated MORB magmas, perhaps due to the presence of metasomatized, isotopically light peridotites in the subcontinental lithospheric mantle (SCLM) source. Although it is possible that $\delta^{56}Fe$ values were slightly modified during seawater alteration and/or metamorphic fluid-rock interactions in some of the eclogites, the impact of fluid-rock interactions on the major element compositions of the eclogites appears to be small. Furthermore, the scarcity of metamorphic veins in the Münchberg Massif argues against significant Fe mobilization in the slab. We suggest that continental eclogites tend to retain their magmatic $\delta^{56}Fe$ values throughout the subduction-exhumation cycle, whereas $\delta^{56}Fe$ values of oceanic eclogites may often be dominated by seafloor alteration with potential local modifications in the slab close to fluid channels. The remarkable robustness of the Fe isotope compositions of continental eclogites suggests that they may be used to reconstruct protolith mantle source properties despite the complex post-magmatic history.

1. Introduction

Iron is a major element in all main reservoirs of the solid Earth, with the special property that it occurs in different valence states (0, +2, and + 3). It largely controls the Earth's redox budget, and conversely, the $Fe^{3+}/\Sigma Fe$ (atomic Fe^{3+} to total Fe ratio) is a useful tracer of redox-dependent processes, for instance, as a direct measure of oxygen fugacity in mantle-derived melts (e.g., Kress and Carmichael, 1991). Notably, $Fe^{3+}/\Sigma Fe$ data from whole rock or glass analyses demonstrate that island arc basalts (IAB) are more oxidized than mid-ocean ridge basalts (MORB; e.g., Christie et al., 1986; Kelley and Cottrell, 2009; Cottrell and Kelley, 2011). This high oxidation state is often explained

* Corresponding author.
E-mail addresses: johannes.pohlner@unifr.ch (J.E. Pohlner), afife.elkorh@unifr.ch (A. El Korh), Massimo.Chiaradia@unige.ch (M. Chiaradia), reiner.klemd@fau.de (R. Klemd), bernard.grobety@unifr.ch (B. Grobéty), pettke@geo.unibe.ch (T. Pettke).

https://doi.org/10.1016/j.chemgeo.2022.120899
Received 20 July 2021; Received in revised form 6 April 2022; Accepted 29 April 2022
Available online 4 May 2022

by mass transfer of oxidized species (e.g., Fe^{3+}, SO_4^{2-}, and CO_3^{2-} are abundant in certain slab lithologies; see Evans and Frost, 2021) from the slab to the mantle wedge by fluids and/or melts (e.g., Evans, 2012; Bénard et al., 2018; Debret et al., 2020). However, the redox systematics of slab-derived fluids and melts are not fully understood, and some recent studies (e.g., Li et al., 2016a; Li et al., 2020; Piccoli et al., 2019) argue that common slab-derived fluids are too reduced to oxidize the mantle wedge. Thus, to improve knowledge about slab redox systematics, more studies on the Fe behavior in high-pressure (HP) rocks are required.

Iron isotopes ($\delta^{x}Fe = [(^{x}Fe/^{54}Fe)_{sample}/(^{x}Fe/^{54}Fe)_{IRMM\text{-}524a\ standard} - 1] \times 1000$ with x = 56 or 57) have proved to be a powerful redox-sensitive tool even in the study of high-temperature processes (e.g., Williams et al., 2009; Williams and Bizimis, 2014; Teng et al., 2011; Nebel et al., 2013, 2015; Dauphas et al., 2017). At equilibrium, the Fe^{3+} species tends to be enriched in heavy Fe isotopes compared to Fe^{2+} (Polyakov and Mineev, 2000; Dauphas et al., 2009, 2014). Since Fe^{3+} is more incompatible than Fe^{2+} during partial mantle melting, basaltic melts are isotopically heavier than their mantle source rocks (Williams et al., 2005; Weyer and Ionov, 2007; Dauphas et al., 2009). However, both basalts and mantle lithologies span a considerable range in $\delta^{56}Fe$ values. The mean $\delta^{56}Fe$ value for mantle peridotite samples (−0.027 ± 0.026‰) suggests a near-chondritic Fe isotope composition of the mantle (Dauphas et al., 2017, and references therein). However, individual samples reveal extreme $\delta^{56}Fe$ values (e.g., as low as −0.69‰), interpreted to reflect kinetic isotope fractionation due to metasomatism during melt percolation (e.g., Williams et al., 2005; Weyer and Ionov, 2007; Zhao et al., 2012; Poitrasson et al., 2013). MORB $\delta^{56}Fe$ values are fairly homogeneous (+0.07 to +0.17‰, mean + 0.105 ± 0.006‰; Weyer and Ionov, 2007; Teng et al., 2013; Sossi et al., 2016), although more extreme compositions were recently reported (+0.03 to +0.36‰; Sun et al., 2020). Back-arc basin basalts (BABB) display $\delta^{56}Fe$ values similar to, or lighter than MORB (−0.01 to +0.18‰; Nebel et al., 2013, 2018; Teng et al., 2013). In contrast, ocean island basalts (OIB) often display heavier $\delta^{56}Fe$ values than MORB (−0.01 to +0.30‰; e.g., Weyer and Ionov, 2007; Teng et al., 2008, 2013; Schuessler et al., 2009; Konter et al., 2016). This range has been explained by lithologically variable mantle sources that are often rich in heavy-$\delta^{56}Fe$ pyroxenites, although mantle source metasomatism and/or high fO_2 during partial melting may also play a role (Williams and Bizimis, 2014; Konter et al., 2016). Contrarily, IAB tend to have lighter $\delta^{56}Fe$ values than MORB (−0.05 to +0.15‰; Dauphas et al., 2009; Nebel et al., 2013, 2015; Foden et al., 2018; Williams et al., 2018). This is thought to be mainly due to repeated previous extraction of heavy-$\delta^{56}Fe$ melts from the mantle source and re-oxidation by sulfate from slab-derived fluids (Nebel et al., 2015; Foden et al., 2018). Direct transfer of isotopically light Fe from the slab to the mantle wedge is still debated: mass balance calculations predict that this process cannot play a dominant role (Nebel et al., 2015; Williams et al., 2018), but its general possibility has been advocated by studies of slab lithologies (Debret et al., 2016, 2018, 2020; Chen et al., 2019). Conversely, presumable recycling of high-$\delta^{56}Fe$ residual slab material into the deep mantle may create isotopically heavy pyroxenite components within the mantle plume sources of OIB (e.g., Konter et al., 2016).

Consequently, subduction zones play a key role in understanding global Fe isotope systematics. Fe mobilization across slab lithologies has been inferred from serpentinites (Debret et al., 2016, 2018, 2020), whiteschists (Chen et al., 2019), and eclogite-derived metamorphic veins (Huang et al., 2020). Most previous studies of subduction-related metabasites focus rather on Fe isotope behavior within specimens (Beard and Johnson, 2004; Li et al., 2016b; Gerrits et al., 2019) or at the outcrop scale (Huang et al., 2020). Regional-scale Fe isotope studies of subducted metabasites are only available from the Ile de Groix, France (El Korh et al., 2017), the Western Alps (Inglis et al., 2017), and the Dabie-Sulu orogen (Yan et al., 2022). These studies suggest a rather conservative behavior of Fe isotopes during subduction, even if pre-subduction hydrothermal alteration may have shifted the $\delta^{56}Fe$ of metabasites (El Korh et al., 2017). More case studies are needed to thoroughly assess how Fe isotopes behave during high-pressure metamorphism. After all, the chemical composition of eclogites results from numerous processes, many of which can cause Fe isotope fractionation:

(1) The parental magmas of most eclogite protoliths are generated by partial melting of the Earth's mantle. Mantle source composition and parameters of partial melting, such as oxygen fugacity and melting degree, can considerably influence the $\delta^{56}Fe$ of the melt (Dauphas et al., 2009; Williams and Bizimis, 2014; Konter et al., 2016; Sossi et al., 2016).
(2) The original Fe isotopic composition of the magma may be changed by processes such as fractional crystallization, wall rock assimilation, or diffusion (see Teng et al., 2008, 2011, 2013; Schuessler et al., 2009; Sossi et al., 2012, 2016; Nebel et al., 2018).
(3) Mafic protoliths, especially those which originated in oceanic spreading centers, are often subjected to alteration by fluids prior to subduction. $\delta^{56}Fe$ values of strongly altered basalts can be drastically raised or lowered (−0.20 to +1.39‰), depending on the redox conditions of alteration-related dissolution-precipitation processes (Rouxel et al., 2003). Isotopically light Fe^{2+} can be leached from rocks while heavy Fe^{3+} is fixed in secondary clays or Fe-hydroxides. By contrast, re-precipitation of Fe^{2+} in sulfides lowers the $\delta^{56}Fe$ of altered mafic rocks (Rouxel et al., 2003). Serpentinization of abyssal peridotites can also cause Fe isotope fractionation at various temperature conditions (El Korh et al., 2020, and references therein).
(4) Experiments (Hill et al., 2010) as well as case studies of serpentinites (Debret et al., 2016, 2018, 2020) and whiteschists (Chen et al., 2019) have proposed that Cl^--bearing, CO_3^{2-}-bearing, and/or SO_4^{2-}-bearing fluids may mobilize Fe^{2+}, thereby preferentially leaching isotopically light Fe from rocks during subduction. By contrast, the only Fe isotope study of eclogite-derived metamorphic veins reported that isotopically heavy Fe was preferentially mobilized because the light Fe was bound by less soluble garnet (Huang et al., 2020). Retrogression may cause local inter-mineral Fe isotope disequilibrium in eclogites without affecting the whole-rock $\delta^{56}Fe$ values (Li et al., 2016b; El Korh et al., 2017; Huang et al., 2020).

Hence, it is necessary to disentangle which of these processes dominantly influence the Fe isotopic composition of eclogites, using fluid-mobile and fluid-immobile elements and other geochemical tools. Here, we present Fe isotope and $Fe^{3+}/\Sigma Fe$ data for 42 eclogite, metagabbro, and paragneiss samples from the Münchberg Massif (Germany), for which major and trace element, and oxygen isotope data have recently been obtained (Pohlner et al., 2021). Eclogite protoliths from the Münchberg Massif appear to be derived from a single mantle source and experienced variable degrees of fractional crystallization, sediment contamination, and fluid-rock interactions (Pohlner et al., 2021), making them well-suited to test the influence of these processes on Fe isotope fractionation.

2. Geologic background and petrography

The Münchberg Massif is an allochthonous nappe pile within the Saxothuringian zone of the Variscan Orogen (e.g., Behr et al., 1982). It records metamorphic events of the Variscan Orogeny, which resulted from the collision of Laurussia and Gondwana during the Devonian and Carboniferous (e.g., Kroner and Romer, 2013; Franke et al., 2017). Its main tectonic units show inverted metamorphic zonation (Fig. 1): from bottom to top, it comprises Paleozoic sedimentary rocks of the Bavarian lithofacies (anchimetamorphic), the Prasinit-Phyllit-Serie (greenschist facies), Randamphibolit-Serie (amphibolite facies), Liegendserie (amphibolite facies), and Hangendserie (Behr et al., 1982; Klemd,

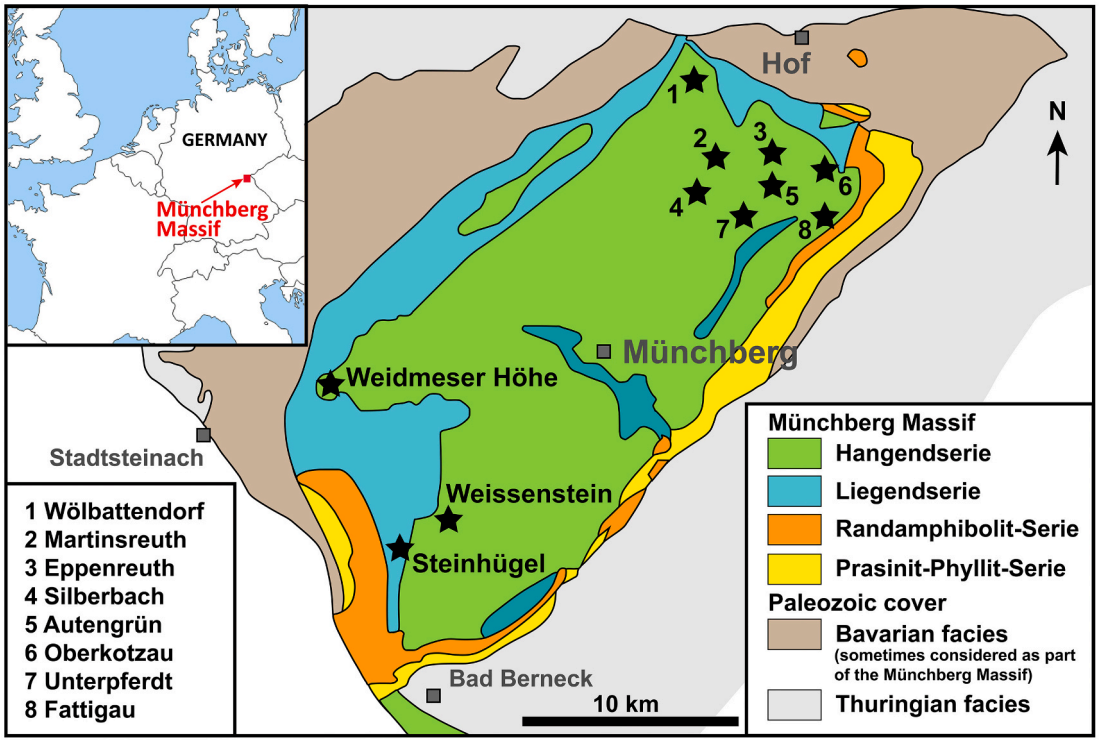

Fig. 1. Geologic map of the Münchberg Massif, modified after Klemd et al. (1991) and Pohlner et al. (2021). Stars represent the sampling localities indicated in Table 1.

2010). A large part of the Hangendserie consists of amphibolites and orthogneisses that are thought to represent bimodal magmatism within a Cadomian arc terrane (Koglin et al., 2018). The numerous eclogite occurrences are located in the lower part of the Hangendserie and in the Hangendserie–Liegendserie boundary, and viewed either as parts of the Hangendserie (e.g., Matthes et al., 1974) or as tectonic bodies (e.g., Stettner, 1960). At the Weissenstein locality, contacts between interlayered eclogites and paragneisses are tectonically undisturbed, suggesting that they formed a volcano-sedimentary sequence that underwent a common tectonometamorphic history (Klemd et al., 1991).

The eclogites of the Münchberg Massif can be classified macroscopically and chemically into dark eclogites (kyanite-free, low Al_2O_3 and Mg# = 100 × Mg/(Mg + Fe^{2+}); atomic %) and light eclogites (kyanite- and/or zoisite-bearing, higher Al_2O_3 and Mg#; Matthes et al., 1974, 1975; Stosch and Lugmair, 1990; Bosbach et al., 1991). The light eclogites are derived from plagioclase-rich cumulate gabbros whereas the dark eclogites mostly represent former basalts (Matthes et al., 1974, 1975; Gebauer and Grünenfelder, 1979; Stosch and Lugmair, 1990; Bosbach et al., 1991; Pohlner et al., 2021). Good correlations between major and immobile trace elements reveal that the dark and light eclogites are derived from a single parental magma through fractional crystallization (Pohlner et al., 2021). The parental magma had a major and trace element composition between those of N-MORB and *E*-MORB (Pohlner et al., 2021). Despite this MORB-like signature and widespread characteristics of low-temperature seawater alteration (positive correlations between Li, B, and Sb contents, and $\delta^{18}O$ values), the eclogite protoliths cannot have formed in a typical oceanic spreading center (Pohlner et al., 2021). This is inferred from petrographic indications that some of the eclogites may have pyroclastic protoliths (Matthes et al., 1974, 1975; Gebauer and Grünenfelder, 1979), and partly low εNd values coupled with high Th/Yb ratios that indicate variable magma contamination by wall-rock sediments (Stosch and Lugmair, 1990). Instead, a more continental setting is suggested, most likely a transitional stage between continental rifting and the opening of the Rheic or Saxothuringian Ocean (Pohlner et al., 2021). This agrees with the late Cambrian to early Ordovician protolith formation age (480 ± 23 Ma, Sm—Nd whole-rock isochron, Stosch and Lugmair, 1990). Sm—Nd and Lu—Hf mineral isochrons (Stosch and Lugmair, 1990; Scherer et al., 2002) constrain eclogite facies metamorphism to between 400 and 380 Ma. The peak metamorphic conditions were estimated by numerous studies, compiled in Massonne and O'Brien (2003) and Liebscher et al. (2007), with temperatures in the range of 550–750 °C (600–650 °C in most studies) and pressures between 20 and 34 kbar, with some studies suggesting ultrahigh-pressure conditions (Okrusch et al., 1991; Klemd et al., 1994; Waizenhöfer, 2017). The adjacent paragneisses contain relics of this HP metamorphism, but underwent extensive amphibolite facies retrogression (Klemd et al., 1991, 1994). This retrogression had a variable effect on the eclogites: observations range from essentially unaffected eclogites and local amphibole/diopside + plagioclase and biotite + plagioclase symplectites around omphacite and phengite to almost complete retrogression (Matthes et al., 1974; Franz et al., 1986). The P-T conditions of symplectite formation were estimated at 8.5–12 kbar and 600 ± 50 °C (Franz et al., 1986). High-pressure and retrograde metamorphism influenced the chemical composition of the eclogites, especially large-ion lithophile element and Pb concentrations, but occasionally more fluid-immobile elements such as Nb and Th may also have been mobilized (Pohlner et al., 2021). However, HP metamorphic veins are scarce at most eclogite localities in the Münchberg Massif, suggesting a limited impact of HP fluid-rock interactions on the bulk rock chemical compositions (Pohlner et al., 2021).

The Liegendserie contains metasediments and orthogneisses, but also metagabbros with largely preserved igneous minerals that are partly replaced by an amphibolite facies paragenesis along grain boundaries (Matthes and Seidel, 1977; Bosbach et al., 1991). The metagabbros and light eclogites are similar in major element composition, both representing former plagioclase-rich cumulates. However, differences in immobile trace element ratios compared to the eclogites demonstrate that the metagabbros are derived from a genetically unrelated igneous suite with an enriched, almost OIB-like parental magma (Pohlner et al., 2021).

For this study, we adopt a chemical distinction of dark, transitional, and light eclogites by means of Al_2O_3 contents and Mg# (Pohlner et al., 2021). The samples used here comprise eighteen dark eclogites, five transitional eclogites, eleven light eclogites, four metagabbros from the Liegendserie, and four paragneisses from the Weissenstein drill core. These samples have been characterized petrographically and chemically by Pohlner et al. (2021), see also Appendix A of the present study.

3. Methods

3.1. Analysis of Fe isotope compositions and Fe speciation

FeO was analyzed volumetrically at the SARM laboratory (CRPG-Nancy), titrating with potassium dichromate after sample dissolution in HF/H_2SO_4 solution. $Fe^{3+}/\Sigma Fe$ ratios of every sample were calculated from volumetric FeO, and $Fe_2O_3^{tot}$ contents from X-ray fluorescence spectrometry (Pohlner et al., 2021). Iron isotope compositions ($\delta^{56}Fe$ and $\delta^{57}Fe$ relative to the IRMM-524a standard) were determined by multi-collector ICP-MS at the Department of Earth Science, University of Geneva, after sample dissolution and column purification. Details are specified in Appendix A.

3.2. Modelling of igneous Fe isotope fractionation

The effect of fractional crystallization on the Fe isotope compositions of the Münchberg eclogite protoliths is modelled here, building upon the cumulate-differentiate mixing model of Pohlner et al. (2021) with a reconstructed primary melt and a cumulate (60 wt% plagioclase, 25 wt % clinopyroxene, 15 wt% olivine, and traces of spinel) as mixing components. Based on the compositions of the eclogite samples that were least affected by fractional crystallization and hydrothermal alteration (Section 5.2), we chose a $\delta^{56}Fe$ value of −0.077‰ for the composition of the initial melt (the magnitude of Fe isotope fractionation does not depend on this choice). Two different models were made, accounting for uncertainties in the initial Fe oxidation state of the melt (see Section 5.1): a $Fe^{3+}/\Sigma Fe$ of 0.15 agrees with the compositions of the least altered and least differentiated Weissenstein eclogite samples (Section 5.2), whereas $Fe^{3+}/\Sigma Fe = 0.10$ (see Appendix) is the revised value for MORB glasses after Berry et al. (2018). This $Fe^{3+}/\Sigma Fe$ ratio (0.10 or 0.15) was kept constant for the whole system (melt + minerals) in every model calculation. Mineral–melt Fe isotope fractionation factors were taken from or estimated based on previous studies. The $\Delta^{56}Fe_{olivine\text{-}melt}$ for basaltic systems is well-constrained (−0.1‰; Sossi et al., 2016). We used the same value for $\Delta^{56}Fe_{clinopyroxene\text{-}melt}$, since clinopyroxene and coexisting olivine in mafic magmas have comparable $\delta^{56}Fe$ values (Chen et al., 2014). The $\Delta^{56}Fe_{plagioclase\text{-}melt}$ is unknown for mafic systems, but plagioclase from felsic systems is isotopically very heavy due to its high $Fe^{3+}/\Sigma Fe$ ratios and low Fe coordination number ($\Delta^{56}Fe_{plagioclase\text{-}magnetite} = +0.4$ to 1.1‰; Wu et al., 2017). However, this effect decreases with increasing anorthite content (Wu et al., 2017) and temperature. We employ a $\Delta^{56}Fe_{plagioclase\text{-}melt}$ of +0.3‰ here. In this context it should be noted that an error in this value would only modestly affect the mass balance due to the low Fe content of plagioclase, e.g., the $\delta^{56}Fe$ value of the cumulate component would be only 0.03‰ higher for a $\Delta^{56}Fe_{plagioclase\text{-}melt}$ of +0.8‰ instead of +0.3‰. The $\Delta^{56}Fe_{spinel\text{-}melt}$ can be estimated based on $\Delta^{56}Fe_{spinel\text{-}olivine}$ values after Polyakov and Mineev (2000). However, this strongly depends on the spinel endmember composition (0.8‰ difference between magnetite and Fe^{2+} spinel at 1100 °C, Polyakov and Mineev, 2000), which can vary broadly depending on the melting degree in the model system. We chose a $\Delta^{56}Fe_{spinel\text{-}melt}$ of +0.3‰, but again, a ± 0.4‰ uncertainty is insignificant for the mass balance due to the low proportion of spinel (<0.3 wt%) among the modelled cumulate minerals. In contrast to magnetite-dominated spinel, ilmenite preferentially incorporates isotopically light Fe (Polyakov and Mineev, 2000), but the incompatible behavior of TiO_2 observed for most of the Münchberg eclogites (Pohlner et al., 2021) contradicts ilmenite fractionation, and ilmenite was never calculated in equilibrium with the melt for <50% crystal fractions. The isotope fractionation factors were kept constant over the cooling interval of ~50 °C, whereas in nature they would increase by 7–8% over such temperature intervals around ~1100 °C, translating into <0.01‰ $\Delta^{56}Fe_{olivine\text{-}melt}$ variation (see Polyakov and Mineev, 2000). For both Fe oxidation states of the initial melt ($Fe^{3+}/\Sigma Fe = 0.15$ and 0.10), the same Fe isotope fractionation factors were used. This simplification is necessary because it is not quantitatively known how the Fe isotope fractionation factors vary with the Fe oxidation state of the melt. Due to very low $Fe^{3+}/\Sigma Fe$ ratios in olivine, $\Delta^{56}Fe_{olivine\text{-}melt}$ may be closer to zero for reduced melts than for oxidized melts.

4. Results

4.1. Fe oxidation state

The $Fe^{3+}/\Sigma Fe$ ratios of the dark eclogites vary between 0.06 and 0.30, without any systematic difference to the transitional and light eclogites (0.09–0.29; Table 1; Fig. 2). The Fe oxidation state is mostly decoupled from major and trace element systematics, including elements like Cr and Zr (Fig. 2a and b) that are strongly sensitive to igneous processes but not to fluid-rock interactions. Weak, but still statistically significant correlations exist between $Fe^{3+}/\Sigma Fe$ and Sb, Cu, and As concentrations (Fig. 2c, e, and f). Two metagabbro samples with pegmatoid textures have $Fe^{3+}/\Sigma Fe$ ratios comparable to those of the eclogites (0.14 and 0.15), and substantially higher than the other two (non-pegmatoid) metagabbros (0.02 and 0.04). The $Fe^{3+}/\Sigma Fe$ values of the paragneisses (0.07–0.10) are within the same range as the most reduced eclogites.

4.2. Fe isotope compositions

Within uncertainties, all the Fe isotope data (Table 1) plot on the mass-dependent theoretical fractionation lines in the $\delta^{57}Fe$ vs. $\delta^{56}Fe$ diagram (Fig. S1). The eclogites mostly display MORB-like $\delta^{56}Fe$ values between +0.00 ± 0.03‰ and + 0.17 ± 0.04‰ (Fig. 3; measurement uncertainties of individual samples are always expressed as 2 × measurement standard error, 2SE). About two thirds of the eclogite samples yielded overlapping 2SE uncertainties. The mean $\delta^{56}Fe$ values of the dark (+0.082 ± 0.017‰), transitional (+0.090 ± 0.021‰), and light eclogites (+0.071 ± 0.022‰) are indistinguishable within 2SE, although the light eclogites tend towards lower values (Fig. 3). For all the eclogites, Fe isotopes do not show strong correlations with any geochemical proxies. Only vague trends with TiO_2 (Fig. 4a), $Fe^{3+}/\Sigma Fe$ (Fig. 4d), and Be (Fig. 4j) were observed.

The $\delta^{56}Fe$ values of the Steinhügel metagabbros (+0.089 ± 0.029‰ to +0.220 ± 0.025‰) are heavier than those of most of the eclogites and fall within the range of MORB and OIB. The pegmatoid metagabbros (STH8 and STH9) are isotopically heavier than the non-pegmatoid samples (STH1 and STH4).

The $\delta^{56}Fe$ values of the Weissenstein paragneisses (+0.028 ± 0.013‰ to +0.096 ± 0.053‰) overlap with those of the eclogites. The mean $\delta^{56}Fe$ (+0.062 ± 0.057‰; 2σ standard deviation) resembles that of the continental crust (+0.07 ± 0.02‰, Poitrasson, 2006; upper continental crust ca. +0.10‰, Foden et al., 2015) as well as modern marine sediments and Proterozoic–Phanerozoic shales (+0.13 ± 0.14‰ and + 0.08 ± 0.30‰, respectively; Beard et al., 2003). Nebel et al. (2015) reported similar $\delta^{56}Fe$ values (+0.05 to +0.12‰) from sediments that are about to enter a subduction zone.

4.3. Model-based prediction of igneous Fe isotope fractionation

The influence of olivine and pyroxene fractionation drives the cumulate component towards a low predicted $\delta^{56}Fe$ value of 0.00‰, while the most differentiated samples (200 μg/g Zr) are predicted to

Table 1
Overview of the samples from the Münchberg Massif used in this study with Fe isotope and Fe3+/ΣFe results.

Sample	locality	rock type	petrologic characteristics	$Fe^{3+}/\Sigma Fe$	δ56Fe (‰)	± 2σ SE (‰)	δ57Fe (‰)	± 2σ SE (‰)	n (Fe isot.)
10.1	Weissenstein drill core	dark eclogite	Fe-Ti-rich MORB-type eclogite	0.15	0.093	0.036	0.134	0.048	8
10.3	Weissenstein drill core	dark eclogite	Fe-Ti-rich MORB-type eclogite	0.13	0.085	0.019	0.119	0.043	5
11.41	Weissenstein drill core	dark eclogite	Fe-Ti-rich MORB-type eclogite	0.18	0.072	0.032	0.099	0.050	5
11.55	Weissenstein drill core	dark eclogite	Fe-Ti-rich MORB-type eclogite	0.22	0.060	0.021	0.083	0.053	5
19.6	Weissenstein drill core	dark eclogite	Fe-Ti-rich MORB-type eclogite	0.12	0.069	0.014	0.086	0.012	5
42.15	Weissenstein drill core	dark eclogite	Fe-Ti-rich MORB-type eclogite	0.24	0.085	0.029	0.126	0.056	5
42.35	Weissenstein drill core	dark eclogite	Fe-Ti-rich MORB-type eclogite	0.18	0.088	0.030	0.130	0.058	5
118.41	Weissenstein drill core	dark eclogite	Fe-Ti-rich MORB-type eclogite	0.15	0.041	0.025	0.064	0.040	8
8_28	Weissenstein	dark eclogite	Fe-Ti-rich MORB-type eclogite	0.16	0.099	0.034	0.161	0.051	9
159	Fattigau	dark eclogite	Fe-Ti-rich MORB-type eclogite	0.27	0.071	0.035	0.113	0.057	7
M1	Fattigau	dark eclogite	Fe-Ti-rich MORB-type eclogite	0.30	0.058	0.038	0.072	0.055	5
FAT1	Fattigau	dark eclogite	Fe-Ti-rich MORB-type eclogite	0.20	0.046	0.033	0.079	0.045	5
FAT2	Fattigau	dark eclogite	Fe-Ti-rich MORB-type eclogite	0.22	0.068	0.032	0.091	0.040	5
FAT6	Fattigau	dark eclogite	Fe-Ti-rich MORB-type eclogite	0.24	0.066	0.044	0.096	0.068	5
UPF2	Unterpferdt	dark eclogite	Fe-Ti-rich MORB-type eclogite	0.06	0.106	0.024	0.158	0.032	12
SIL4	Silberbach	dark eclogite	Fe-Ti-rich MORB-type eclogite	0.10	0.165	0.042	0.261	0.087	3
ATG5	Autengrün	dark eclogite	Fe-Ti-rich MORB-type eclogite	0.18	0.118	0.025	0.161	0.054	4
ATG17	Autengrün	dark eclogite	Fe-Ti-rich MORB-type eclogite	0.17	0.078	0.021	0.130	0.045	4
0.13	Weissenstein drill core	transitional eclogite	moderately Al-Mg-rich eclogite	0.16	0.084	0.019	0.130	0.031	5
0.35	Weissenstein drill core	transitional eclogite	moderately Al-Mg-rich eclogite	0.14	0.081	0.035	0.123	0.042	5
WEI3	Weissenstein	transitional eclogite	moderately Al-Mg-rich eclogite	0.26	0.061	0.043	0.101	0.050	3
SIL1	Silberbach	transitional eclogite	moderately Al-Mg-rich eclogite	0.09	0.122	0.035	0.176	0.058	10
MR2	Martinsreuth	transitional eclogite	moderately Al-Mg-rich eclogite	0.09	0.100	0.014	0.145	0.026	9
WEI	Weissenstein	light eclogite	kyanite-bearing Al-Mg-rich eclogite	0.20	0.041	0.034	0.066	0.056	5
S1861	Oberkotzau	light eclogite	kyanite-bearing Al-Mg-rich eclogite	0.13	0.096	0.020	0.123	0.045	4
S1864	Oberkotzau	light eclogite	kyanite-bearing Al-Mg-rich eclogite	0.15	0.070	0.040	0.093	0.048	8
Ober 1	Oberkotzau	light eclogite	kyanite-bearing Al-Mg-rich eclogite	0.18	0.001	0.032	−0.004	0.054	7
Ober 2	Oberkotzau	light eclogite	kyanite-bearing Al-Mg-rich eclogite	0.17	0.049	0.044	0.063	0.069	7
Ober 3	Oberkotzau	light eclogite	kyanite-bearing Al-Mg-rich eclogite	0.29	0.107	0.021	0.152	0.027	8
SIL6B	Silberbach	light eclogite	kyanite-bearing Al-Mg-rich eclogite	0.09	0.105	0.031	0.162	0.047	9
ATG2	Autengrün	light eclogite	kyanite-bearing Al-Mg-rich eclogite	0.20	0.061	0.014	0.091	0.035	4
EPP2	Eppenreuth	light eclogite	kyanite-bearing Al-rich eclogite	0.13	0.073	0.021	0.118	0.055	4
WBD1	Wölbattendorf	light eclogite	kyanite-bearing Al-Mg-rich eclogite	0.12	0.108	0.027	0.162	0.041	9
86.54	Weissenstein drill core	paragneiss	metapelite to metapsammite	0.07	0.028	0.013	0.038	0.045	3
87	Weissenstein drill core	paragneiss	metapelite to metapsammite	0.09	0.068	0.044	0.097	0.087	3
148.3	Weissenstein drill core	paragneiss	metapelite to metapsammite	0.10	0.096	0.053	0.148	0.089	6
154.01	Weissenstein drill core	paragneiss	metapelite to metapsammite	0.07	0.054	0.004	0.086	0.043	3
STH1	Steinhügel (Liegendserie)	metagabbro	amphibolite facies coronas around relict igneous phases	0.04	0.089	0.029	0.130	0.046	3
STH4	Steinhügel (Liegendserie)	metagabbro	amphibolite facies coronas around relict igneous phases	0.02	0.095	0.023	0.146	0.040	7
STH8	Steinhügel (Liegendserie)	meta-quartz diorite	pegmatoidal; consists of amphibolite facies pseudomorphs	0.15	0.163	0.018	0.251	0.043	3
STH9	Steinhügel (Liegendserie)	meta-quartz diorite	pegmatoidal; consists of amphibolite facies pseudomorphs	0.14	0.220	0.025	0.330	0.014	3

have a $\delta^{56}Fe$ value of +0.11‰ or + 0.13‰ (with $Fe^{3+}/\Sigma Fe$ ratios of 0.15 and 0.10, respectively, for the initial melt). A positive correlation between Zr and $\delta^{56}Fe$ is predicted by the model, but our eclogite sample set does not show such a correlation (Fig. 4f). The choice of the initial $Fe^{3+}/\Sigma Fe$ ratio of the melt (0.10 or 0.15) seems to have only little influence on the total Fe isotope fractionation between cumulate and melt, but this is uncertain because it is not known quantitatively how mineral-melt Fe isotope fractionation factors vary with oxygen fugacity. In contrast, the modelled $Fe^{3+}/\Sigma Fe$ ratios of the cumulate (down to 0.07 or 0.12, respectively) and differentiate (0.12 or 0.17, respectively) endmembers depend on the initial $Fe^{3+}/\Sigma Fe$ (0.10 or 0.15) of the melt. In both cases, modelled $Fe^{3+}/\Sigma Fe$ ratios increase with progressive differentiation, but such a correlation is not observed for our eclogite dataset (Fig. 2b).

5. Discussion

5.1. Controls on Fe oxidation state

The range in $Fe^{3+}/\Sigma Fe$ ratios of the eclogites (0.06–0.30) substantially exceeds that of fresh MORB, for which different estimates exist, using different analytical methods (0.07 ± 0.01, Christie et al., 1986; 0.12 ± 0.02, Bézos and Humler, 2005; 0.16 ± 0.01, Cottrell and Kelley, 2011; 0.10 ± 0.02, Berry et al., 2018). Our modelling predicts that for unmodified mafic protoliths, $Fe^{3+}/\Sigma Fe$ and Zr should be correlated due to $Fe^{3+}/\Sigma Fe$ changes during fractional crystallization (Fig. 2b). In absence of notable seawater alteration, such original magmatic $Fe^{3+}/\Sigma Fe$ ratios, correlating with differentiation proxies, can be preserved in eclogites (Aulbach et al., 2017, 2019). However, our samples do not show a correlation between $Fe^{3+}/\Sigma Fe$ and Zr, suggesting that the whole-rock $Fe^{3+}/\Sigma Fe$ is not dominated by fractional crystallization. Variations

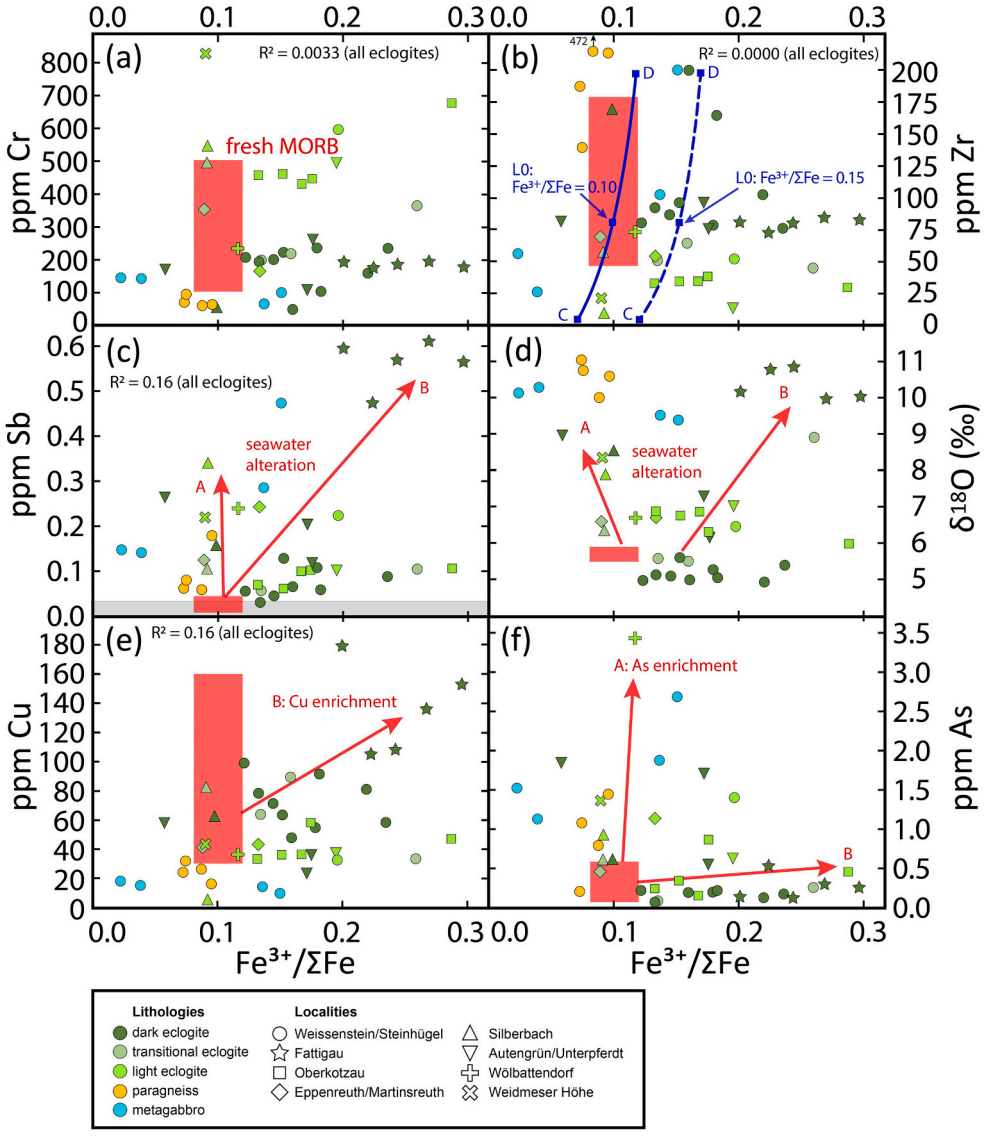

Fig. 2. $Fe^{3+}/\Sigma Fe$ ratios of samples from the Münchberg Massif, compared to selected geochemical data from Pohlner et al. (2021). Reference fields for fresh MORB are constructed after Berry et al. (2018) for $Fe^{3+}/\Sigma Fe$, Harmon and Hoefs (1995) for $\delta^{18}O$, and Jenner and O'Neill (2012); limited to weakly differentiated samples, see Pohlner et al., 2021) for element concentrations. The R^2 values indicate the quality of correlations (for all eclogites, correlations with $R^2 > 0.11$ are statistically significant at a significance level of 0.05). The lines in (b) illustrate the predicted $Fe^{3+}/\Sigma Fe$ evolution obtained from fractional crystallization modelling (Section 3.2) with the initial melt (L0), cumulate (C), and differentiate (D) compositions. The gray baseline band in (c) represents the average detection limit of Sb. Arrows indicate qualitative evolution lines, with A and B suggesting two contrasting styles of fluid-rock interactions as discussed in Section 5.1.

in mantle source composition and partial melting alone cannot explain the $Fe^{3+}/\Sigma Fe$ data of the Münchberg eclogites because they span a larger range than those of fresh MORB samples from various localities worldwide (Cottrell and Kelley, 2011). Furthermore, rock geochemical systematics imply a single parental magma for all the eclogites, and that seawater alteration affected most of the rocks (Pohlner et al., 2021). Consequently, we suggest that many of the Münchberg eclogites were significantly oxidized during fluid-rock interactions, whereas some may have been slightly reduced. The $Fe^{3+}/\Sigma Fe$ signatures do not correlate with $\delta^{18}O$ values and only weakly so with Sb contents, both of which are seawater alteration proxies (Fig. 2c and d). However, this does not contradict seawater alteration, which commonly comprises different alteration stages with contrasting influences on element contents, oxygen isotope compositions, and Fe oxidation states of the rocks (e.g., Alt and Honnorez, 1984). Contrasting alteration styles are indeed suggested for the Fattigau eclogites on the one hand (high Sb and Cu contents, $\delta^{18}O$ values, and $Fe^{3+}/\Sigma Fe$ ratios; low As contents; Fig. 2) and the remaining eclogites on the other hand (intermediate Sb contents and $\delta^{18}O$ values; MORB-like $Fe^{3+}/\Sigma Fe$ ratios; low Cu contents; high As contents; Fig. 2) with the exception of the Weissenstein eclogites, which appear to be mostly unaffected by seawater alteration (Pohlner et al., 2021). It is unclear whether this reflects two contrasting stages of seawater alteration, or uniform seawater alteration that was locally overprinted by metamorphic fluid-rock interactions. In any case, contrasting patterns for $Fe^{3+}/\Sigma Fe$, Cu, As, and Sb suggest at least two different modes of fluid-rock interactions, likely with contrasting redox conditions.

Care needs to be taken when interpreting absolute values of titration-derived $Fe^{3+}/\Sigma Fe$ data, which can overestimate the actual $Fe^{3+}/\Sigma Fe$ ratio of the rock due to air contamination (O'Neill et al., 1993). Our dataset may be affected by this to some degree as the eclogite samples that are least affected by seawater alteration have $Fe^{3+}/\Sigma Fe$ ratios around 0.15, somewhat higher than the most recent estimate (0.10 ± 0.02) for fresh MORB (Berry et al., 2018). On the other hand, the eclogite protoliths were not formed in a typical mid-ocean ridge setting but most likely in a rift-drift transition setting (Pohlner et al., 2021), thus it cannot be excluded that the parental magma may have been somewhat more oxidized than a typical MORB magma. For the metagabbros, the $Fe^{3+}/\Sigma Fe$ ratios of samples STH1 (0.04) and STH4 (0.02) are so low that they can hardly be overestimated. The pegmatoid metagabbro samples are more oxidized, but Matthes and Seidel (1977) and Bosbach et al. (1991) also found that many of their (non-pegmatoid) metagabbro samples are strongly reduced. Our fractional crystallization model predicts that cumulate rocks have lower $Fe^{3+}/\Sigma Fe$ ratios than their differentiated counterparts (Fig. 2b), similar to the metagabbro trend. On the other hand, given that the metagabbros have high $\delta^{18}O$ values and Sb concentrations (Fig. 2c and d), hydrothermal alteration may have

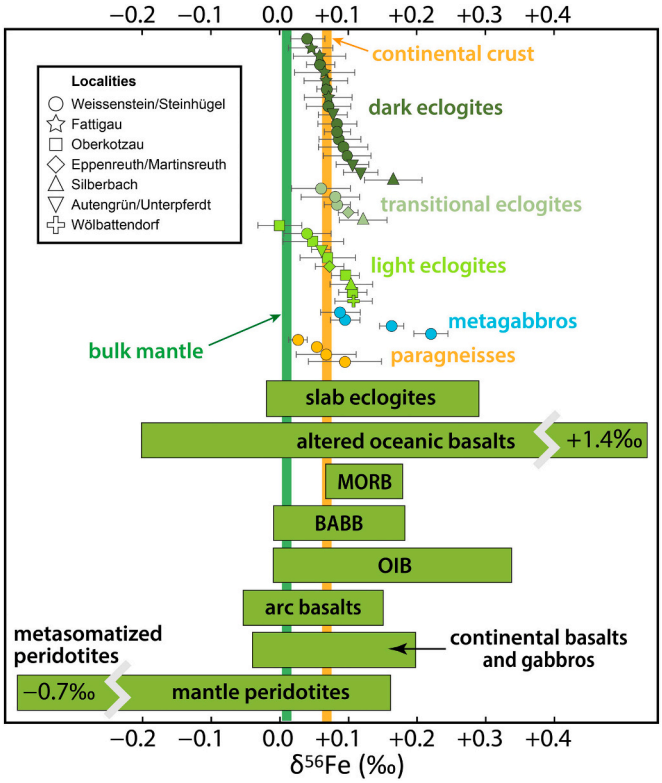

Fig. 3. Fe isotope compositions of samples from the Münchberg Massif (error bars represent 2SE), compared to terrestrial reference reservoirs. The vertical lines represent the compositions of bulk mantle (Weyer and Ionov, 2007) and continental crust (Poitrasson, 2006). Horizontal bars represent the total range of sample compositions available in the literature for subduction-related eclogites (El Korh et al., 2017; Inglis et al., 2017; Huang et al., 2020), altered oceanic basalts (Rouxel et al., 2003), MORB (Sossi et al., 2016), BABB (Nebel et al., 2013, 2018), OIB (Teng et al., 2013; Konter et al., 2016), arc basalts (Dauphas et al., 2009; Nebel et al., 2013; Foden et al., 2018), continental basalts and gabbros (Craddock and Dauphas, 2011; Sossi et al., 2012; Chen et al., 2014; Nebel et al., 2020), and mantle peridotites (Weyer and Ionov, 2007; Poitrasson et al., 2013; Zhao et al., 2012, 2015).

affected the $Fe^{3+}/\Sigma Fe$ ratios of the metagabbros, similar to some of the eclogites. However, the metagabbro data set is too small to permit robust conclusions regarding the cause of their low $Fe^{3+}/\Sigma Fe$ ratios.

5.2. Fe isotope compositions of the igneous and sedimentary protoliths

The Fe isotopic compositions of rock samples can be influenced by process-driven fractionation effects as well as variable source components. Due to typically high Fe concentrations in mafic rocks, the protolith $\delta^{56}Fe$ values are expected to be robust unless sufficiently intense metasomatic processes were involved. A rather conservative behavior of Fe in the Münchberg eclogites seems likely because (1) they display fairly uniform $\delta^{56}Fe$ values in the range of fresh MORB, and continental basalts and gabbros (Fig. 3), and (2) the positive correlation between $Fe_2O_3^{tot}$ and Zr concentrations (Pohlner et al., 2021) shows very little scatter, suggesting an undisturbed magmatic relationship between the two elements. However, for complete preservation of the igneous protoliths' Fe isotope compositions, our fractional crystallization model predicts correlations between $\delta^{56}Fe$ values and concentrations of fluid-immobile elements that are typically enriched/depleted during igneous fractionation (e.g., TiO_2, Zr, and Cr; Fig. 4). Such correlations are not obvious in our data (Fig. 4), although the majority of our samples agree with the modelled trends within error. The strongest correlations of $\delta^{56}Fe$ values with any geochemical indices are with $Fe^{3+}/\Sigma Fe$ (Fig. 4d) and Be (Fig. 4j), but even these correlations are weak and thus do not provide strong evidence for any specific geological process. The positive correlation between Be and $\delta^{56}Fe$ values is consistent with the incompatible behavior of Be during fractional crystallization and low Be mobility in metamorphic fluids (Ryan, 2002), but this leaves the question why the $\delta^{56}Fe$ values do not correlate with the other immobile, incompatible trace elements. Although Be and Zr are similarly incompatible during the differentiation of tholeiitic magmas (Ryan, 2002), the two elements are not correlated in the eclogite data (Pohlner et al., 2021), suggesting that Be behavior in our sample set is probably more complex. We note that, although fluid-immobile elements except Be do not correlate with Fe isotopes, they correlate well with each other, advocating that all the eclogite protoliths were derived from a single parental magma (Pohlner et al., 2021). Thus, $\delta^{56}Fe$ variations due to variable partial melting fractions (ca. 0.04‰; Konter et al., 2016; Sossi et al., 2016) or mantle oxygen fugacities (up to 0.1‰; Konter et al., 2016) are unlikely. Instead, the expected correlations may be obscured by analytical uncertainties, or blurred by modest $\delta^{56}Fe$ modifications during fluid-rock interactions (see Section 5.3). Additionally, it may be possible that the modelled Fe isotope fractionation during fractional crystallization is overestimated, e.g., due to incomplete knowledge of the mineral-melt Fe isotope fractionation factors.

When considering only the eclogite samples from the Weissenstein locality, which are mostly unaffected by seawater alteration (Pohlner et al., 2021), strong correlations with fluid-immobile elements are similarly absent. This is not surprising, given that the range of $\delta^{56}Fe$ values in this sample subset is small compared to analytical uncertainties. Based on geochemical criteria, some of the Weissenstein eclogite samples (10.1, 10.3, 19.6, 42.15, 42.35, and 118.41) appear to be little affected by fractional crystallization (no Eu anomalies and close to 8 wt% MgO, 275 μg/g Cr, and 80 μg/g Zr; see Pearce, 2014) and seawater alteration (MORB-like $Fe^{3+}/\Sigma Fe$, $\delta^{18}O$, Li, B, and Sb). These samples yield a mean $\delta^{56}Fe$ value of $+0.077 \pm 0.016$‰ (2SE) which we interpret as the Fe isotope composition of the parental magma after emplacement in the upper crust, indistinguishable from the mean $\delta^{56}Fe$ value of the entire eclogite sample set ($+0.080 \pm 0.010$‰; 2SE). Despite the likely continental origin of the eclogites (Pohlner et al., 2021), these mean values are comparable to the average $\delta^{56}Fe$ value of primitive (Mg# = 70–75) MORB magmas ($+0.06 \pm 0.01$‰, Sossi et al., 2016), but lower than the mean $\delta^{56}Fe$ value of MORB samples ($+0.105 \pm 0.006$‰; Teng et al., 2013). Most MORB samples have higher $\delta^{56}Fe$ values than primitive MORB magmas because they experienced fractional crystallization especially of olivine, as suggested by Mg# <70 (Sossi et al., 2016). The six aforementioned Weissenstein samples have Mg# of 60–62, suggesting that the parental magma represented by these samples had already lost olivine crystals before emplacement and fractionation in the upper crust. MORB samples with Mg# = 60–62 have $\delta^{56}Fe$ values between 0.08‰ and 0.14‰ (Sossi et al., 2016), mostly higher than the Münchberg eclogite mean. This suggests that the primitive precursor magma of the Münchberg eclogites possibly had a slightly lighter Fe isotope composition than typical primitive MORB magmas. We recall that despite geochemical characteristics that greatly resemble those of MORB, the Münchberg eclogites were probably formed in a different geologic setting, likely a shallow-water transitional stage between continental rifting and seafloor spreading (Pohlner et al., 2021). In such a setting, basaltic melts may be sourced from the subcontinental lithospheric mantle (SCLM), which is often subjected to metasomatic processes (e.g., Zhao et al., 2015). The average Fe isotope compositions of SCLM xenoliths and abyssal peridotites are comparable (Sossi et al., 2016), but metasomatism by melt percolation often generates extreme $\delta^{56}Fe$ values in SCLM peridotites (−0.69 to +0.10‰; Zhao et al., 2012, 2015; Poitrasson et al., 2013). These extreme Fe isotope compositions may mostly cancel out each other when a magma body is assembled from a larger mantle volume. However, if a small contribution from preferential melting of isotopically light mantle lithologies is provided, isotopically light parental magmas may be generated. Apart from active margins, iron isotope data for continental basalts (Craddock and

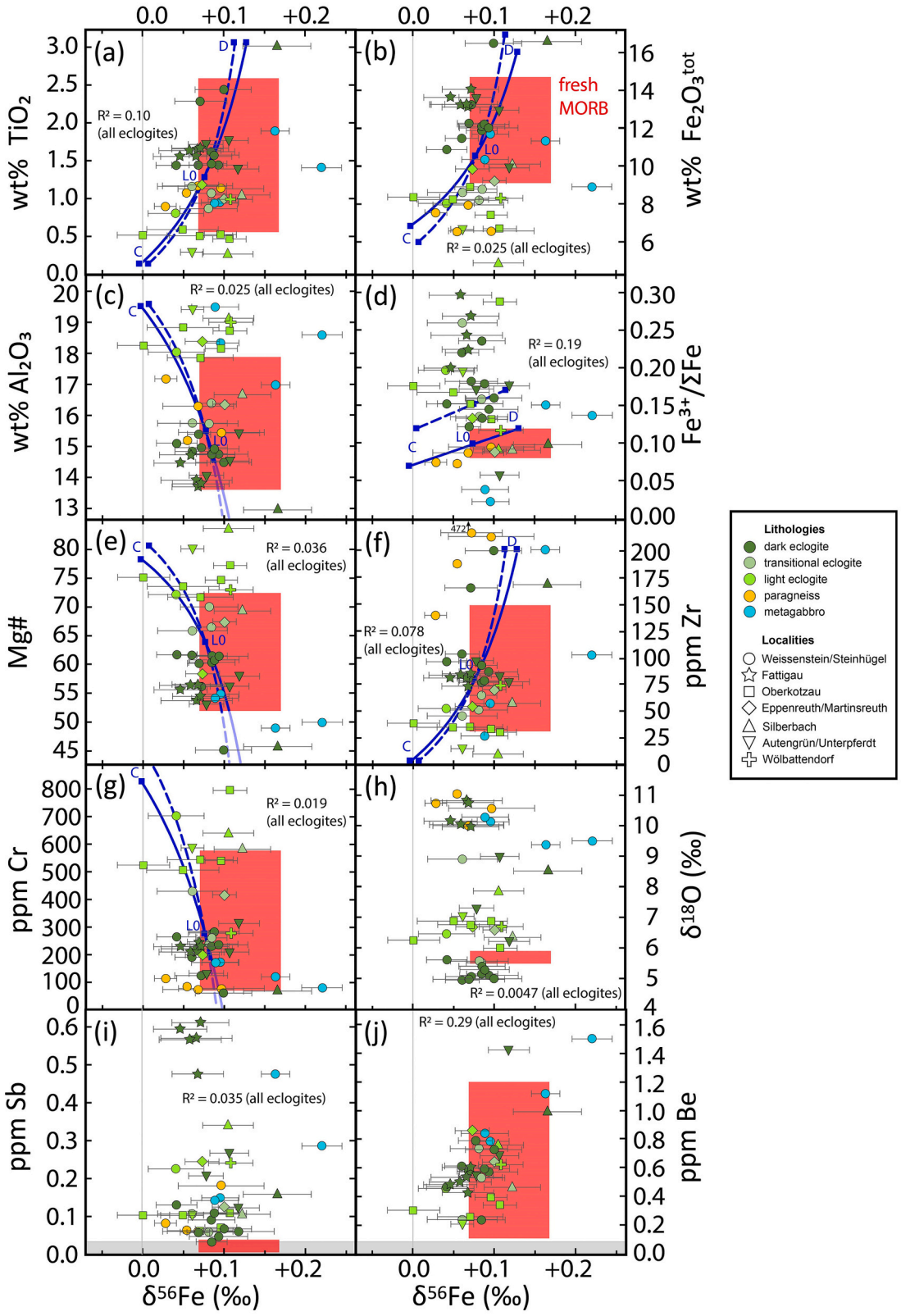

Fig. 4. Fe isotopic compositions of samples from the Münchberg Massif, compared to selected major and trace element contents reported in Pohlner et al. (2021). Error bars represent measurement uncertainties (2SE). Reference compositions for fresh MORB are constructed after Sossi et al. (2016) for δ^{56}Fe, Harmon and Hoefs (1995) for δ^{18}O, Berry et al. (2018) for $Fe^{3+}/\Sigma Fe$, and Jenner and O'Neill, 2012; limited to weakly differentiated samples, see Pohlner et al., 2021) for element concentrations. The R^2 values are reported to indicate the quality of correlations (for all eclogites, correlations with $R^2 > 0.11$ are statistically significant at a significance level of 0.05). The lines in (a-g) illustrate the predicted δ^{56}Fe evolution obtained from fractional crystallization modelling (Section 3.2) with the initial melt (L0 with $Fe^{3+}/\Sigma Fe = 0.10$ represented by the continuous line, and $Fe^{3+}/\Sigma Fe = 0.15$ represented by the dashed line), cumulate (C), and differentiate (D) compositions. In (c), (e), and (g), the lines representing the model calculations are partly pale to indicate that extrapolation towards differentiated compositions becomes unreliable for compatible elements. The gray baseline bands in (i) and (j) display average detection limits.

Dauphas, 2011, and the BCR samples of Weyer and Ionov, 2007, and Li et al., 2019) and gabbros (Sossi et al., 2012; Chen et al., 2014; Nebel et al., 2020) are scarce, and additional data may reveal whether the Fe isotope compositions of some continental mafic rocks reflect mantle metasomatism.

The Steinhügel metagabbros yielded δ^{56}Fe values that are MORB-like, or slightly heavier. This is consistent with their more enriched, almost OIB-like mantle source (see Pohlner et al., 2021). In contrast to the eclogites, the metagabbros often show correlations between δ^{56}Fe values and fractional crystallization proxies, as the pegmatoid metagabbros are isotopically heavier than the non-pegmatoid metagabbros. However, based on only four analyses, it is difficult to judge whether the igneous Fe isotope signature is preserved. Given that these samples yielded high δ^{18}O values (+9.4 to +10.1‰; Pohlner et al., 2021), fluid-rock interactions may have modified their Fe isotope compositions.

The Weissenstein paragneisses have δ^{56}Fe values comparable to those of typical sedimentary protoliths (see Section 4.2). Although this similarity suggests preservation of the protolith Fe isotope compositions, modifications during diagenesis and/or fluid-rock interactions in the slab cannot be excluded. The δ^{56}Fe values of the paragneisses differ from those of the eclogites by $\leq$0.1‰, with $Fe_2O_3^{tot}$ contents that are lower than in most of the eclogites (Fig. 4b). Hence, even though the trace element compositions of many eclogite protoliths were modified by a few percent of magma contamination by the paragneiss protoliths (Stosch and Lugmair, 1990; Pohlner et al., 2021), this contamination has a negligible effect on the δ^{56}Fe values of the eclogites.

5.3. Fe isotope behavior during fluid-rock interactions

Fluid-rock interactions potentially inducing variations in the Fe isotope compositions of eclogites may have taken place either during seawater alteration and/or during later subduction zone metamorphism. Given the high Fe concentrations in mafic protoliths, significant δ^{56}Fe modifications by fluid-rock interactions require high Fe isotope fractionation factors, influx of Fe with extreme isotopic compositions, and/or high fluid/rock ratios combined with significant fluid Fe mobility. Seawater alteration appears to have affected most of the Münchberg eclogite protoliths (Pohlner et al., 2021), and is generally capable of causing strong Fe isotope fractionation (Rouxel et al., 2003). However, the samples of Rouxel et al. (2003) are much more oxidized than our samples, and many of them experienced drastic changes in major element compositions. This is in strong contrast with our samples, which essentially retained their original compositions regarding most major elements (Pohlner et al., 2021), including Fe (Section 5.2). The small deviations of the δ^{56}Fe values of the eclogites from their expected igneous values also advocate limited Fe mobility. A minor effect of fluid-rock interactions on the Fe isotope compositions is possible, and may explain the lack of clear correlations as stated in Section 5.2. At least the eclogites from the Fattigau locality experienced oxidation and Cu enrichment during fluid-rock interactions (Section 5.1). While this might also happen without any Fe mobility, the Fattigau eclogites yielded δ^{56}Fe values (mean = +0.062 ± 0.009‰) that are lower than those of most of the other dark eclogites, and up to 0.005‰ below their model-predicted igneous values (Fig. 4). Hence, it can be envisaged that the type of fluid-rock interaction that is geochemically suggested only for the Fattigau locality included addition of isotopically light Fe, or removal of isotopically heavy Fe. Given that the Fattigau eclogites have the heaviest oxygen isotope compositions of all eclogites in our data set (Fig. 4h), we suggest this effect to be related to seawater alteration, but cannot exclude later subduction-related fluid-rock interactions as the cause. In contrast to the Fattigau locality, some of the light and transitional eclogites have δ^{56}Fe values higher than those expected by the fractional crystallization model. All of these eclogites appear to have experienced some degree of seawater alteration (elevated δ^{18}O values and Sb contents, Fig. 4h and i). This may have included minor addition of isotopically heavy Fe, or removal of isotopically light Fe. Due to the relatively low Fe contents of the light eclogites, their δ^{56}Fe values can be shifted more easily than those of the Fe-rich dark eclogites from the same localities.

Whereas seawater alteration in eclogites needs to be inferred from geochemical information alone (see Pohlner et al., 2021), metamorphic fluid-rock interactions can be assessed based additionally on textural information. Textural and geochemical evidence of alteration generated by prograde-derived pervasive fluid flow along grain boundaries is commonly overprinted, or limited to a small scale, and, thus, to localized element transport. Based on regional studies of metabasites of different facies, it was inferred that Fe isotope compositions remain constant during prograde dehydration, reflecting the typically low solute content of prograde fluids (El Korh et al., 2017; Inglis et al., 2017; Yan et al., 2022). In contrast, close to peak conditions, significant major and trace element changes were reported for the alteration aureoles surrounding eclogite-facies dehydration veins, which may contain high-variance mineral assemblages and, thus, represent major conduits of channelized high fluid flow during prograde HP metamorphism in blueschists and eclogites (e.g., Klemd, 2013). Thus, significant fluid flow-associated element scavenging and transport under eclogite-facies conditions is typically channelized, and only the alteration aureoles (which are usually a few centimeters to decimeters thick) around transport veins undergo substantial chemical modification by externally-derived (i.e. non-rock-buffered) fluids (e.g., Zack and John, 2007). In contrast, internal fluids generated by dehydration are rock-buffered, and the stability of Fe-bearing HP minerals in such systems limits Fe mobility (El Korh et al., 2017). Although Cl-rich fluids can dissolve some Fe^{2+} (Hill et al., 2010), mass balance calculations predict that the release of aqueous fluids by eclogite dehydration cannot alter the Fe isotope composition of the eclogite significantly at ca. 600 °C (Inglis et al., 2017). The Münchberg eclogites probably experienced higher temperatures around 700 °C (Waizenhöfer, 2017), where Fe solubilities could be somewhat higher, and according to Liebscher et al. (2007), conditions for water-saturated melting of eclogite may have been reached. In an eclogite-vein system in the Dabie Orogen that experienced P-T conditions comparable to the Münchberg Massif, Fe isotope fractionation between a vein-forming dehydration fluid and the adjacent eclogite (with <0.1‰ δ^{56}Fe change in the eclogite) was reported and explained by preferential dissolution of high-δ^{56}Fe omphacite and epidote from the eclogites (Huang et al., 2020). In the Münchberg Massif, however, HP veins are rare at most localities and do not form large interconnected networks, indicating rather fluid-poor systems in absence of lawsonite dehydration as a fluid source (Pohlner et al., 2021). It seems that due to limited HP fluid flow in an eclogite paragenesis which effectively stored Fe, the Fe isotope compositions of the Münchberg eclogites probably did not change significantly during HP metamorphism. This might be different for the rare vein-bearing eclogites in the Münchberg Massif, but these require a separate study.

Retrogression variably affected the Münchberg eclogites, and symplectite abundance partly correlates with Ba and Pb concentrations, suggesting influx of metasediment-equilibrated fluids (Pohlner et al., 2021). While Ba and Pb are highly concentrated in the gneisses and very mobile in fluids, it is much more difficult to imagine that these fluids transported enough Fe to shift the δ^{56}Fe values of the eclogites significantly. The most retrogressed eclogite samples (e.g., ATG5 and EPP2) do not show any anomalous Fe isotope compositions, arguing against a notable role of retrogression for bulk-rock Fe isotope compositions.

5.4. Significance for the global Fe isotope cycle

Implications for global Fe isotope systematics need to consider that the Münchberg Massif is not representative for typical subducted oceanic crust due to its continental context. Typical oceanic crustal rocks often undergo a much more intense seawater alteration than that recorded in the Münchberg eclogites, including prominent shifts in major element compositions (e.g., Alt and Honnorez, 1984). This may

commonly cause significant pre-subduction Fe isotope fractionation, as demonstrated by the study of Rouxel et al. (2003). Such a thorough hydration of the oceanic crust also increases its potential for later fluid-rock interactions in the slab, which may include Fe mobilization. Where such Fe mobilization during eclogite dehydration was demonstrated, it was found that the fluids tend to be enriched in isotopically heavy Fe released by preferential dissolution of high-$Fe^{3+}/\Sigma Fe$ phases like omphacite, and thus cannot cause the low $\delta^{56}Fe$ values of IAB (Huang et al., 2020). More investigations of the Fe isotope and $Fe^{3+}/\Sigma Fe$ systematics of slab lithologies are necessary to identify the cause of the high oxidation state of IAB.

6. Conclusions

1. The Münchberg eclogites seem to have approximately preserved their igneous Fe isotope compositions, despite their complex history involving seawater alteration followed by subduction to eclogite facies conditions. We suggest that this immobile behavior of Fe during fluid-rock interactions is typical at least for continental eclogites, which often lack strong pre-subduction alteration and thus store too little water to form interconnected vein networks upon dehydration.
2. The $\delta^{56}Fe$ value of the primitive parental magma of the eclogite protoliths was probably slightly lower than those of primitive MORB magmas. This may reflect a contribution of isotopically light, metasomatized SCLM peridotite during magma generation, which is plausible for the likely genesis of the Münchberg parental magmas in a transitional stage between continental rifting and the opening of the Rheic or Saxothuringian Ocean.
3. Despite the mostly conservative behavior of Fe in the Münchberg eclogites, minor $\delta^{56}Fe$ modifications during fluid-rock interactions might have taken place, possibly during seawater alteration and/or (less likely) in the slab. Oceanic eclogites, which often experienced strong seafloor alteration before subduction, probably cover a larger range in $\delta^{56}Fe$ values than the Münchberg eclogites due to seafloor alteration-related Fe isotope fractionation. In the vicinity of external fluid channels, further modifications of the Fe isotope compositions during subduction are conceivable for oceanic eclogites. In contrast, continental eclogites appear to be robust against post-magmatic $\delta^{56}Fe$ modifications, hence Fe isotopes may even prove useful for reconstructing their mantle source properties.

Declaration of Competing Interest

The authors declare that they have no known competing financial interests or personal relationships that could have appeared to influence the work reported in this paper.

Acknowledgments

Samples 19.6 and MR2 were provided by the rock archive of the Chair for Geodynamics and Geomaterial Research, University of Würzburg (Ulrich Schüßler). The column chemistry for Fe isotope analysis was performed by Michèle Senn. The helpful and constructive reviews by Sonja Aulbach and John Foden, and previous comments by Stéphanie Duchêne and one anonymous reviewer on an earlier version, are gratefully acknowledged, as well as the editorial handling by Catherine Chauvel. The research was funded by the Swiss National Science Foundation (Grant 200021_178947).

Appendix A. Supplementary data

Supplementary data to this article can be found online at https://doi.org/10.1016/j.chemgeo.2022.120899.

References

Alt, J.C., Honnorez, J., 1984. Alteration of the upper oceanic crust, DSDP site 417: mineralogy and chemistry. Contrib. Mineral. Petrol. 87, 149–169.
Aulbach, S., Woodland, A.B., Vasilyev, P., Galvez, M.E., Viljoen, K.S., 2017. Effects of low-pressure igneous processes and subduction on Fe3+/ΣFe and redox state of mantle eclogites from Lace (Kaapvaal craton). Earth Planet. Sci. Lett. 474, 283–295.
Aulbach, S., Woodland, A.B., Stern, R.A., Vasilyev, P., Heaman, L.M., Viljoen, K.S., 2019. Evidence for a dominantly reducing Archaean ambient mantle from two redox proxies, and low oxygen fugacity of deeply subducted oceanic crust. Scientific reports, 9(1), 1-11.Evidence for a dominantly reducing Archaean ambient mantle from two redox proxies, and low oxygen fugacity of deeply subducted oceanic crust. Sci. Rep. 9, 20190.
Beard, B.L., Johnson, C.M., 2004. Inter-mineral Fe isotope variations in mantle-derived rocks and implications for the Fe geochemical cycle. Geochim. Cosmochim. Acta 68, 4727–4743.
Beard, B.L., Johnson, C.M., Von Damm, K.L., Poulson, R.L., 2003. Iron isotope constraints on Fe cycling and mass balance in oxygenated Earth oceans. Geology 31, 629–632.
Behr, H.J., Engel, W., Franke, W., 1982. Variscan wildflysch and nappe tectonics in the Saxothuringian Zone (Northeast Bavaria, West Germany). Am. J. Sci. 282, 1438–1470.
Bénard, A., Klimm, K., Woodland, A.B., Arculus, R.J., Wilke, M., Botcharnikov, R.E., Shimizu, N., Nebel, O., Rivard, C., Ionov, D.A., 2018. Oxidising agents in sub-arc mantle melts link slab devolatilisation and arc magmas. Nat. Commun. 9, 1–10.
Berry, A.J., Stewart, G.A., O'Neill, H.S.C., Mallmann, G., Mosselmans, J.F.W., 2018. A re-assessment of the oxidation state of iron in MORB glasses. Earth Planet. Sci. Lett. 483, 114–123.
Bézos, A., Humler, E., 2005. The $Fe^{3+}/\Sigma Fe$ ratios of MORB glasses and their implications for mantle melting. Geochim. Cosmochim. Acta 69, 711–725.
Bosbach, D., Stosch, H.G., Seidel, E., 1991. Magmatic and metamorphic evolution of metagabbros in the Münchberg Massif, NE Bavaria. Contrib. Mineral. Petrol. 107, 112–123.
Chen, L.M., Song, X.Y., Zhu, X.K., Zhang, X.Q., Yu, S.Y., Yi, J.N., 2014. Iron isotope fractionation during crystallization and sub-solidus re-equilibration: constraints from the Baima mafic layered intrusion, SW China. Chem. Geol. 380, 97–109.
Chen, Y.X., Lu, W., He, Y., Schertl, H.P., Zheng, Y.F., Xiong, J.W., Zhou, K., 2019. Tracking Fe mobility and Fe speciation in subduction zone fluids at the slab-mantle interface in a subduction channel: a tale of whiteschist from the Western Alps. Geochim. Cosmochim. Acta 267, 1–16.
Christie, D.M., Carmichael, I.S.E., Langmuir, C.H., 1986. Oxidation states of mid-ocean ridge basalt glasses. Earth Planet. Sci. Lett. 79, 397–411.
Cottrell, E., Kelley, K.A., 2011. The oxidation state of Fe in MORB glasses and the oxygen fugacity of the upper mantle. Earth Planet. Sci. Lett. 305, 270–282.
Craddock, P.R., Dauphas, N., 2011. Iron isotopic compositions of geological reference materials and chondrites. Geostand. Geoanal. Res. 35, 101–123.
Dauphas, N., Craddock, P.R., Asimow, P.D., Bennett, V.C., Nutman, A.P., Ohnenstetter, D., 2009. Iron isotopes may reveal the redox conditions of mantle melting from Archean to present. Earth Planet. Sci. Lett. 288, 255–267.
Dauphas, N., Roskosz, M., Alp, E.E., Neuville, D.R., Hu, M.Y., Sio, C.K., Tissot, F.L.H., Zhao, J., Tissandier, L., Médard, E., Cordier, C., 2014. Magma redox and structural controls on iron isotope variations in Earth's mantle and crust. Earth Planet. Sci. Lett. 398, 127–140.
Dauphas, N., John, S.G., Rouxel, O., 2017. Iron isotope systematics. Rev. Mineral. Geochem. 82, 415–510.
Debret, B., Millet, M.A., Pons, M.L., Bouilhol, P., Inglis, E., Williams, H., 2016. Isotopic evidence for iron mobility during subduction. Geology 44, 215–218.
Debret, B., Bouilhol, P., Pons, M.L., Williams, H., 2018. Carbonate transfer during the onset of slab devolatilization: new insights from Fe and Zn stable isotopes. J. Petrol. 59, 1145–1166.
Debret, B., Reekie, C.D.J., Mattielli, N., Beunon, H., Ménez, B., Savov, I.P., Williams, H. M., 2020. Redox transfer at subduction zones: insights from Fe isotopes in the Mariana forearc. Geochem. Perspect. Lett. 12, 46–51.
El Korh, A., Luais, B., Deloule, E., Cividini, D., 2017. Iron isotope fractionation in subduction-related high-pressure metabasites (Ile de Groix, France). Contrib. Mineral. Petrol. 172, 41.
El Korh, A., Boiron, M.C., Cividini, D., 2020. A multi-isotope study (Fe, Ge, O) of hydrothermal alteration in the Limousin ophiolite (French Massif Central). Lithos 378–379, 105876.
Evans, K.A., 2012. The redox budget of subduction zones. Earth-Sci. Rev. 113, 11–32.
Evans, K.A., Frost, B.R., 2021. Deserpentinization in subduction zones as a source of oxidation in arcs: a reality check. J. Petrol. 62, 1–32.
Foden, J., Sossi, P.A., Wawryk, C.M., 2015. Fe isotopes and the contrasting petrogenesis of A-, I-and S-type granite. Lithos 212, 32–44.
Foden, J., Sossi, P.A., Nebel, O., 2018. Controls on the iron isotopic composition of global arc magmas. Earth Planet. Sci. Lett. 494, 190–201.
Franke, W., Cocks, L.R.M., Torsvik, T.H., 2017. The Palaeozoic Variscan oceans revisited. Gondwana Res. 48, 257–284.
Franz, G., Thomas, S., Smith, D.C., 1986. High-pressure phengite decomposition in the Weissenstein eclogite, Münchberger Gneiss Massif, Germany. Contrib. Mineral. Petrol. 92, 71–85.
Gebauer, D., Grünenfelder, M., 1979. U-Pb zircon and Rb-Sr mineral dating of eclogites and their country rocks. Example: Münchberg Gneiss Massif, Northeast Bavaria. Earth Planet. Sci. Lett. 42, 35–44.
Gerrits, A.R., Inglis, E.C., Dragovic, B., Starr, P.G., Baxter, E.F., Burton, K.W., 2019. Release of oxidizing fluids in subduction zones recorded by iron isotope zonation in garnet. Nat. Geosci. 12, 1029–1033.

Harmon, R.S., Hoefs, J., 1995. Oxygen isotope heterogeneity of the mantle deduced from global 18 O systematics of basalts from different geotectonic settings. Contrib. Mineral. Petrol. 120, 95–114.
Hill, P.S., Schauble, E.A., Young, E.D., 2010. Effects of changing solution chemistry on Fe3+/Fe2+ isotope fractionation in aqueous Fe–Cl solutions. Geochim. Cosmochim. Acta 74, 6669–6689.
Huang, J., Guo, S., Jin, Q.Z., Huang, F., 2020. Iron and magnesium isotopic compositions of subduction-zone fluids and implications for arc volcanism. Geochim. Cosmochim. Acta 278, 376–391.
Inglis, E.C., Debret, B., Burton, K.W., Millet, M.A., Pons, M.L., Dale, C.W., Bouihol, P., Cooper, M., Nowell, G.M., McCoy-West, A., Williams, H.M., 2017. The behaviour of iron and zinc stable isotopes accompanying the subduction of mafic oceanic crust: a case study from Western Alpine Ophiolites. Geochem. Geophys. Geosyst. https://doi.org/10.1002/2016GC006735.
Jenner, F.E., O'Neill, H.S.C., 2012. Analysis of 60 elements in 616 ocean floor basaltic glasses. Geochem. Geophys. Geosyst. 13, Q02005. https://doi.org/10.1029/2011GC004009.
Kelley, K.A., Cottrell, E., 2009. Water and the oxidation state of subduction zone magmas. Science 325, 605–607.
Klemd, R., 2010. Early Variscan allochthonous domains: The Münchberg Complex, Frankenberg, Wildenfels, and Góry Sowie. In: Linnemann, U., Romer, R.L. (Eds.), Pre-Mesozoic Geology of Saxo-Thuringia: From the Cadomian Active Margin to the Variscan Orogen. Schweizerbart, Stuttgart, pp. 221–232.
Klemd, R., 2013. Metasomatism during high-pressure metamorphism: Eclogites and blueschist-facies rocks. In: Harlov, D.E., Austrheim, H. (Eds.), Metasomatism and the Chemical Transformation of Rock. Springer, Berlin, Heidelberg, pp. 351–413.
Klemd, R., Matthes, S., Okrusch, M., 1991. High-pressure relics in meta-sediments intercalated with the Weissenstein eclogite, Münchberg gneiss complex, Bavaria. Contrib. Mineral. Petrol. 107, 328–342.
Klemd, R., Matthes, S., Schüssler, U., 1994. Reaction textures and fluid behaviour in very high pressure calc-silicate rocks of the Münchberg gneiss complex, Bavaria, Germany. J. Metamorph. Geol. 12, 735–745.
Koglin, N., Zeh, A., Franz, G., Schüssler, U., Glodny, J., Gerdes, A., Brätz, H., 2018. From Cadomian magmatic arc to Rheic Ocean closure: the geochronological-geochemical record of nappe protoliths of the Münchberg Massif, NE Bavaria (Germany). Gondwana Res. 55, 135–152.
Konter, J.G., Pietruszka, A.J., Hanan, B.B., Finlayson, V.A., Craddock, P.R., Jackson, M. G., Dauphas, N., 2016. Unusual δ^{56}Fe values in Samoan rejuvenated lavas generated in the mantle. Earth Planet. Sci. Lett. 450, 221–232.
Kress, V.C., Carmichael, I.S.E., 1991. The compressibility of silicate liquids containing Fe 2 O 3 and the effect of composition, temperature, oxygen fugacity and pressure on their redox states. Contrib. Mineral. Petrol. 108, 82–92.
Kroner, U., Romer, R.L., 2013. Two plates – many subduction zones: the Variscan orogeny reconsidered. Gondwana Res. 24, 298–329.
Li, J.L., Gao, J., Klemd, R., John, T., Wang, X.-S., 2016a. Redox processes in subducting oceanic crust recorded by sulfide-bearing high-pressure rocks and veins (SW Tianshan, China). Contrib. Mineral. Petrol. 171, 72. https://doi.org/10.1007/s00410-016-1284-2.
Li, D.Y., Xiao, Y.L., Li, W.Y., Zhu, X., Williams, H.M., Li, Y.L., 2016b. Iron isotopic systematics of UHP eclogites respond to oxidizing fluid during exhumation. J. Metamorph. Geol. 34, 987–997.
Li, J., Tang, S.H., Zhu, X.K., Li, Z.H., Li, S.Z., Yan, B., Wang, Y., Sun, J., Shi, Y., Dong, A., Belshaw, N.S., Zhang, X., Liu, A., Liu, J., Wang, D., Jiang, S., Hou, K., Cohen, A.S., 2019. Basaltic and solution reference materials for iron, copper and zinc isotope measurements. Geostand. Geoanal. Res. 43, 163–175.
Li, J.L., Schwarzenbach, E.M., John, T., Ague, J.J., Huang, F., Gao, J., Klemd, R., Whitehouse, M.J., Wang, X.-S., 2020. Uncovering and quantifying the subduction zone sulfur cycle from the slab perspective. Nat. Commun. 11, 1–12.
Liebscher, A., Franz, G., Frei, D., Dulski, P., 2007. High-pressure melting of eclogite and the P–T–X history of tonalitic to trondhjemitic zoisite-pegmatites, Münchberg Massif, Germany. J. Petrol. 48, 1001–1019.
Massonne, H.J., O'Brien, P.J., 2003. The Bohemian massif and the NW Himalaya. In: Carswell, D.A., Compagnoni, R. (Eds.), Ultra-High Pressure Metamorphism. Eur. Mineral. Union Notes Mineral., vol. 5, pp. 145–188.
Matthes, S., Seidel, E., 1977. Die Eklogitvorkommen des kristallinen Grundgebirges in NE-Bayern, X. Bestehen genetische Beziehungen zwischen Eklogit und Meta-Gabbro innerhalb des Münchberger Gneisgebietes? Neues Jahrb. Mineral. Abh. 129, 269–291.
Matthes, S., Richter, P., Schmidt, K., 1974. Die Eklogitvorkommen des kristallinen Grundgebirges in NE-Bayern. VII. Ergebnisse einer Kernbohrung durch den Eklogitkörper des Weißensteins. Neues Jahrb. Mineral. Abh. 120, 270–314.
Matthes, S., Richter, P., Schmidt, K., 1975. Die Eklogitvorkommen des kristallinen Grundgebirges in NE-Bayern. IX. Petrographie, Geochemie und Petrogenese der Eklogite des Münchberger Gneisgebietes. Neues Jahrb. Mineral. Abh. 126, 45–86.
Nebel, O., Arculus, R.J., Sossi, P.A., Jenner, F.E., Whan, T.H.E., 2013. Iron isotopic evidence for convective resurfacing of recycled arc-front mantle beneath back-arc basins. Geophys. Res. Lett. 40, 5849–5853.
Nebel, O., Sossi, P.A., Bénard, A., Wille, M., Vroon, P.Z., Arculus, R.J., 2015. Redox-variability and controls in subduction zones from an iron-isotope perspective. Earth Planet. Sci. Lett. 432, 142–151.
Nebel, O., Sossi, P.A., Foden, J., Bénard, A., Brandl, P.A., Stammeier, J.A., Lupton, J., Richter, M., Arculus, R.J., 2018. Iron isotope variability in ocean floor lavas and mantle sources in the Lau back-arc basin. Geochim. Cosmochim. Acta 241, 150–163.
Nebel, O., Sossi, P.A., Ivanic, T.J., Bénard, A., Gardinier, N.J., Langford, R.L., Arculus, R. J., 2020. Incremental growth of layered mafic-ultramafic intrusions through melt replenishment into a crystal mush zone traced by Fe-Hf isotope systematics. Front. Earth Sci. 8 https://doi.org/10.3389/feart.2020.00002.
Okrusch, M., Matthes, S., Klemd, R., O'Brien, P.J., Schmidt, K., 1991. Eclogites at the northwestern margin of the Bohemian Massif: a review. Eur. J. Mineral. 3, 707–730.
O'Neill, H.S.C., Rubie, D.C., Canil, D., Geiger, C.A., Ross, C.R., Seifert, F., Woodland, A. B., 1993. Ferric iron in the upper mantle and in transition zone assemblages: implications for relative oxygen Fugacities in the mantle. Geophys. Monogr. Ser. 74, 73–88.
Pearce, J.A., 2014. Immobile element fingerprinting of ophiolites. Elements 10, 101–108.
Piccoli, F., Hermann, J., Pettke, T., Connolly, J.A.D., Kempf, E.D., Vieira Duarte, J.F., 2019. Subducting serpentinites release reduced, not oxidized, aqueous fluids. Sci. Rep. 9, 19573.
Pohlner, J.E., El Korh, A., Klemd, R., Grobéty, B., Pettke, T., Chiaradia, M., 2021. Trace element and oxygen isotope study of eclogites and associated rocks from the Münchberg Massif (Germany) with implications on the protolith origin and fluid-rock interactions. Chem. Geol. 579, 120352.
Poitrasson, F., 2006. On the iron isotope homogeneity level of the continental crust. Chem. Geol. 235, 195–200.
Poitrasson, F., Delpech, G., Grégoire, M., 2013. On the iron isotope heterogeneity of lithospheric mantle xenoliths: implications for mantle metasomatism, the origin of basalts and the iron isotope composition of the Earth. Contrib. Mineral. Petrol. 165, 1243–1258.
Polyakov, V.B., Mineev, S.D., 2000. The use of Mössbauer spectroscopy in stable isotope geochemistry. Geochim. Cosmochim. Acta 64, 849–865.
Rouxel, O., Dobbek, N., Ludden, J., Fouquet, Y., 2003. Iron isotope fractionation during oceanic crust alteration. Chem. Geol. 202, 155–182.
Ryan, J.G., 2002. Trace-element systematics of beryllium in terrestrial materials. Rev. Mineral. Geochem. 50, 121–145.
Scherer, E.E., Mezger, K., Münker, C., 2002. Lu-Hf ages of high-pressure metamorphism in the Variscan fold belt of southern Germany. Geochim. Cosmochim. Acta 66, A677.
Schuessler, J.A., Schoenberg, R., Sigmarsson, O., 2009. Iron and lithium isotope systematics of the Hekla volcano, Iceland - evidence for Fe isotope fractionation during magma differentiation. Chem. Geol. 258, 78–91.
Sossi, P.A., Foden, J.D., Halverson, G., 2012. Redox-controlled iron isotope fractionation during magmatic differentiation. Contrib. Mineral. Petrol. 164, 757–772.
Sossi, P.A., Nebel, O., Foden, J.D., 2016. Iron isotope systematics in planetary reservoirs. Earth Planet. Sci. Lett. 452, 295–308.
Stettner, G., 1960. Über Bau und Entwicklung der Münchberger Gneismasse. Geol. Rundsch. 49, 350–375.
Stosch, H.G., Lugmair, G.W., 1990. Geochemistry and evolution of MORB-type eclogites from the Münchberg Massif, southern Germany. Earth Planet. Sci. Lett. 99, 230–249.
Sun, P., Niu, Y., Guo, P., Duan, M., Chen, S., Gong, H., Wang, X., Xiao, Y., 2020. Large iron isotope variation in the eastern Pacific mantle as a consequence of ancient low-degree melt metasomatism. Geochim. Cosmochim. Acta 286, 269–288.
Teng, F.Z., Dauphas, N., Helz, R.T., 2008. Iron isotope fractionation during magmatic differentiation in Kilauea Iki Lava Lake. Science 320, 1620–1622.
Teng, F.Z., Dauphas, N., Helz, R.T., Gao, S., Huang, S., 2011. Diffusion-driven magnesium and iron isotope fractionation in Hawaiian olivine. Earth Planet. Sci. Lett. 308, 317–324.
Teng, F.Z., Dauphas, N., Huang, S., Marty, B., 2013. Iron isotopic systematics of oceanic basalts. Geochim. Cosmochim. Acta 107, 12–26.
Waizenhöfer, F., 2017. Evolution of Rocks from the Münchberg Metamorphic Complex (NE Bavaria). Unpublished PhD thesis. University of Stuttgart, 183 pp.
Weyer, S., Ionov, D.A., 2007. Partial melting and melt percolation in the mantle: the message from Fe isotopes. Earth Planet. Sci. Lett. 259, 119–133.
Williams, H.M., Bizimis, M., 2014. Iron isotope tracing of mantle heterogeneity within the source regions of oceanic basalts. Earth Planet. Sci. Lett. 404, 396–407.
Williams, H.M., Peslier, A.H., McCammon, C., Halliday, A.N., Levasseur, S., Teutsch, N., Burg, J.P., 2005. Systematic iron isotope variations in mantle rocks and minerals: the effects of partial melting and oxygen fugacity. Earth Planet. Sci. Lett. 235, 435–452.
Williams, H.M., Nielsen, S.G., Renac, C., Griffin, W.L., O'Reilly, S.Y., McCammon, C.A., Pearson, N., Viljoen, F., Alt, J.C., Halliday, A.N., 2009. Fractionation of oxygen and iron isotopes by partial melting processes: implications for the interpretation of stable isotope signatures in mafic rocks. Earth Planet. Sci. Lett. 283, 156–166.
Williams, H.M., Prytulak, J., Woodhead, J.D., Kelley, K.A., Brounce, M., Plank, T., 2018. Interplay of crystal fractionation, sulfide saturation and oxygen fugacity on the iron isotope composition of arc lavas: an example from the Marianas. Geochim. Cosmochim. Acta 226, 224–243.
Wu, H., He, Y., Bao, L., Zhu, C., Li, S., 2017. Mineral composition control on inter-mineral iron isotopic fractionation in granitoids. Geochim. Cosmochim. Acta 198, 208–217.
Yan, Q., He, Y., Zhu, C., Wu, H., Shi, Q., 2022. Reduction of iron with no systematic isotope fractionation during continental subduction observed in metamorphic rocks from the Dabie-Sulu orogen, China. J. Asian Earth Sci. 225, 105054.
Zack, T., John, T., 2007. An evaluation of reactive fluid flow and trace element mobility in subducting slabs. Chem. Geol. 239, 199–216.
Zhao, X., Zhang, H., Zhu, X., Tang, S., Yan, B., 2012. Iron isotope evidence for multistage melt–peridotite interactions in the lithospheric mantle of eastern China. Chem. Geol. 292, 127–139.
Zhao, X.M., Zhang, H.F., Zhu, X.K., Zhu, B., Cao, H.H., 2015. Effects of melt percolation on iron isotopic variation in peridotites from Yangyuan, North China Craton. Chem. Geol. 401, 96–110.